A novel method for determining the gap-state profile and its application to amorphous $Si_{1-x}Ge_x$:H films

Hideharu Matsuura
Electrotechnical Laboratory, 1-1-4 Umezono, Tsukuba, Ibaraki 305, Japan

(Received 16 February 1988; accepted for publication 6 May 1988)

A novel technique has been proposed for determining the density-of-state (DOS) distribution in the energy gap of highly resistive amorphous semiconductors, using amorphous/crystalline heterojunction structures. The technique has been tested and applied to undoped hydrogenated amorphous silicon (a-Si:H) films and silicon-germanium (a-$Si_{1-x}Ge_x$:H) alloy films, covering the optical gap (E_0) range of 1.3–1.7 eV. For undoped a-Si:H with $E_0 = 1.7$ eV, the peak of the midgap DOS distribution has been located at 0.84 eV below the conduction-band mobility edge, E_C, with a value of 2×10^{15} cm^{-3} eV^{-1}. For undoped a-$Si_{1-x}Ge_x$:H ($E_0 = 1.44$ eV), the same has been obtained at 0.70 eV below E_C, with a magnitude of 7×10^{16} cm^{-3} eV^{-1}. Those midgap DOS have been found to be correlated with singly occupied dangling bonds, representative of a homogeneous bulk property of the material, unaffected by interface states.

I. INTRODUCTION

The optoelectronic properties of hydrogenated amorphous silicon (a-Si:H) films are critically linked with the density and distribution of localized states in the mobility gap of a-Si:H. In order to enhance the performance of a-Si:H based devices, such as solar cells and thin-film transistors, a low density-of-state (DOS) distribution, $g(E)$, in the mobility gap, is essential. Measurement of $g(E)$ and an understanding of the nature of the gap states are, therefore, very important. The problem has received considerable attention, and many techniques have been developed to determine $g(E)$. These include both optical and electrical methods.

Photoacoustic spectroscopy (PAS),[1–4] photothermal deflection spectroscopy (PDS),[5,6] and constant photocurrent measurements (CPM)[7] give the variation of the optical absorption coefficient (α) versus the photon energy ($h\nu$) in the material. The number of defects is related to the absorption. However, the optical absorption coefficient is associated with a joint density of the initial and final states. Therefore, in general, it is rather difficult to distinguish one from the other.

Transient capacitance methods like deep-level transient spectroscopy (DLTS)[8–10] and isothermal capacitance transient spectroscopy (ICTS)[11,12] are tested techniques for determining the density of states in a-Si:H. However, these methods are limited in their application to doped samples of low resistivity. For high resistivity materials, such as undoped or compensated a-Si:H films, the dielectric relaxation times are too long for the measurement of the capacitance which can reflect the depletion width of the junction.

While modulated photocurrent methods (MPC)[13,14] give information on the DOS peak position above the Fermi level for highly resistive undoped a-Si:H, an estimation of the actual density of gap states is difficult. Space-charge-limited current (SCLC) measurements[15–17] do give a quantitative estimation of $g(E)$, but only above the Fermi level. However, the determination of $g(E)$ below the Fermi level for undoped films is important as well, because gap states located below the Fermi level would also determine the optoelectronic properties of the film and would, therefore, affect the performance of devices based on these films.

In the present work, the author has tried to determine $g(E)$ below the Fermi level in undoped a-Si:H films and also in undoped hydrogenated amorphous silicon-germanium alloy (a-$Si_{1-x}Ge_x$:H) films, the importance of the latter arising from this variety being the low band-gap component in tandem-type amorphous silicon solar cells.

Prior to this, by using undoped (i.e., n-type) a-Si:H/p-type crystalline silicon (p c-Si) heterojunctions under high frequency (100 kHz),[18] an effective density of donorlike states (N_I) for a-Si:H and its electron affinity (χ) was obtained. The analytical approach there had been that the capacitance of a-Si:H becomes equal to the geometric capacitance of the a-Si:H film due to its longer dielectric relaxation time, while that of c-Si is associated with the depletion width of c-Si which reflects the space charge of the depletion region of a-Si:H. This method will be called a heterojunction-monitored capacitance (HMC) method in the following sections. The HMC method has been applied to undoped a-$Si_{1-x}Ge_x$:H with the optical gap (E_0) between 1.3 and 1.6 eV.

It has been demonstrated that the $g(E)$ below the Fermi level of amorphous films ($1.3\ \text{eV} \leqslant E_0 \leqslant 1.7$ eV) can be determined from the experimental results involving transient as well as temperature-dependent measurements. First, analyses of steady-state and transient HMC methods will be mentioned, followed by a discussion on the experimental determination of undoped a-Si:H and undoped a-$Si_{1-x}Ge_x$:H.

II. THEORY OF HETEROJUNCTION-MONITORED CAPACITANCE METHOD

A. Steady-state regime of HMC

The depletion region formed by an undoped a-Si:H (or a-$Si_{1-x}Ge_x$:H)/p-type c-Si heterojunction is considered. When a reverse dc voltage (V_{DC}) is applied, it produces space-charge layers both in amorphous and crystalline semiconductors. Under the assumption that this p c-Si has only shallow acceptors, the space charge in the p c-Si is formed by

 0021-8979/88/161964-10$02.40

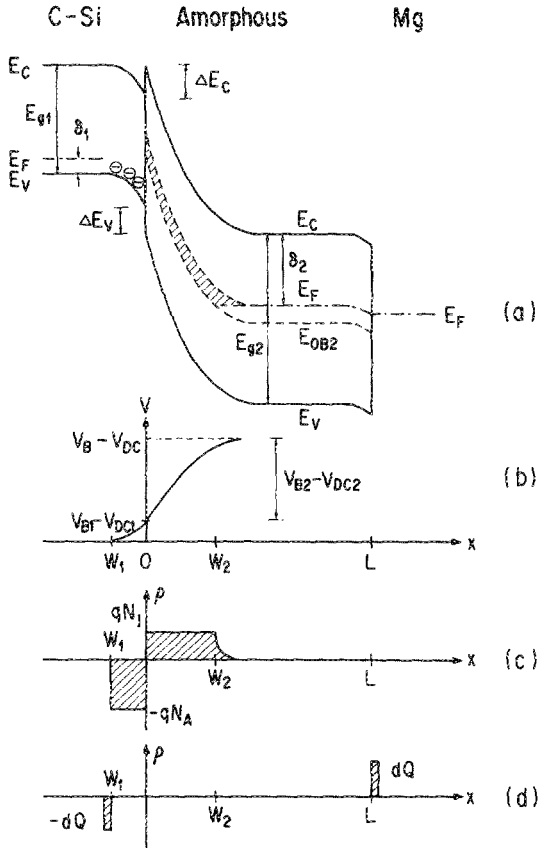

FIG. 1. Schematic sketches of the heterojunction: (a) energy-band diagram; (b) potential variation; (c) space-charge density for a reverse dc voltage; (d) charge in response to a small 1-MHz ac voltage to measure capacitance. The gap states as indicated by the hatched area of (a) are positively charged states. Dashed-dotted lines represent the Fermi level. ⊖ represents negatively charged acceptors in the depletion region.

negatively charged acceptors. However, the amorphous component possesses gap states. Origin of the space charge in amorphous semiconductors is schematically discussed. In the neutral region, all the gap states below the Fermi level (E_F) are occupied by electrons, while in the depletion region the states above E_{OB2} as indicated by the hatched area in Fig. 1(a) are vacant of electrons, where E_{OB2} is determined by thermal-emission rates for electrons and holes for gap states to the extended states and given by

$$E_{OB2} = E_C - \frac{E_{g2}}{2} + \left(\frac{kT}{2}\right) \ln\left(\frac{\nu_p}{\nu_n}\right). \tag{1}$$

Here ν_p and ν_n are the attempt-to-escape frequencies for holes and electrons, respectively (see Appendix A). Therefore, the gap states in the hatched area in Fig. 1(a) behave like positively charged states, here, referred to as donorlike states, and the density of the donorlike states is constant between spatial position 0 and W_2.[19] This, together with the density of donors (if they exist), gives the effective density of donorlike states (N_I), as shown in Fig. 1(c). Figure 1(b) shows the potential variation with distance where V_B is the built-in potential. The depletion widths (W_1 and W_2) are given by

$$qN_A W_1 \simeq qN_I W_2 , \tag{2}$$

with

$$W_1 = \sqrt{2\epsilon_{s1}(V_{B1} - V_{DC1})/qN_A} \tag{3}$$

and

$$W_2 = \sqrt{2\epsilon_{s2}(V_{B2} - V_{DC2})/qN_I} . \tag{4}$$

Here N_A is the density of the acceptors in p c-Si and ϵ_s is the semiconductor permittivity. In Fig. 1, δ indicates the distance in energy from the Fermi level to the nearest band edge, E_g is the energy gap of the semiconductor, W is the depletion width, L is the thickness of the amorphous film, and ΔE is the difference in energy between band edges of the two semiconductors. The subscripts 1 and 2 refer to p c-Si and undoped a-Si:H (or a-$Si_{1-x}Ge_x$:H), respectively, and the subscripts C and V refer to the conduction and valence bands, respectively.

The capacitance has been measured using a small ac voltage of 1 MHz. The resistivity (ρ_1) of p c-Si used in this study is lower than 10 Ω cm so that the dielectric relaxation time ($\epsilon_{s1}\rho_1$) becomes 10^{-11} s, indicating that the redistribution of holes (majority carriers of p c-Si) can respond to the 1-MHz ac voltage. The capacitance (C_1) in c-Si is given by

$$C_1 = \epsilon_{s1}/W_1 . \tag{5}$$

On the other hand, the minimum value of resistivity (ρ_2) for undoped a-$Si_{1-x}Ge_x$:H used is 10^7 Ω cm. Then, the dielectric relaxation time becomes 10^{-5} s, sugggesting that the redistribution of electrons (majority carriers of those films) cannot respond to an ac voltage higher than 100 kHz. Thus, the undoped film may be considered as a dielectric material in its behavior in the case of the 1-MHz ac voltage, indicating that the capacitance (C_2) in a-Si:H (or a-$Si_{1-x}Ge_x$:H) should be given by

$$C_2 = \epsilon_{s2}/L . \tag{6}$$

The measured HMC (C_{HM}) at 1 MHz is from a series of C_1 and C_2, and is expressed as

$$\frac{1}{C_{HM}} = \frac{1}{C_1} + \frac{1}{C_2}, \tag{7}$$

because spatially the redistribution of charged carriers can respond to the 1-MHz ac voltage at W_1 and L, as shown in Fig. 1(d). From Eqs. (2)–(4), the following relation is obtained:

$$(V_{B1} - V_{DC1})/(V_{B2} - V_{DC2}) \simeq N_I\epsilon_{s2}/N_A\epsilon_{s1} . \tag{8}$$

The final equation is obtained as

$$W_1^2 = \epsilon_{s1}^2 (1/C_{HM} - 1/C_2)^2 \tag{9}$$

$$\simeq 2\epsilon_{s1}\epsilon_{s2}N_I(V_B - V_{DC})/qN_A(N_A\epsilon_{s1} + N_I\epsilon_{s2}) , \tag{10}$$

from Eqs. (3), (5), (7), and (8). As is clear from Eq. (10), the values of N_I and V_B can be graphically determined from the slope and the intercept of the abscissa, respectively.

B. Transient regime of HMC

In order to estimate $g(E)$, the transient HMC is considered after a reverse-bias dc voltage (V_{DC}) is applied to the sample over the zero-bias condition, as shown in Fig. 2. At $t = +0$, V_{DC} is applied across the whole of the amorphous

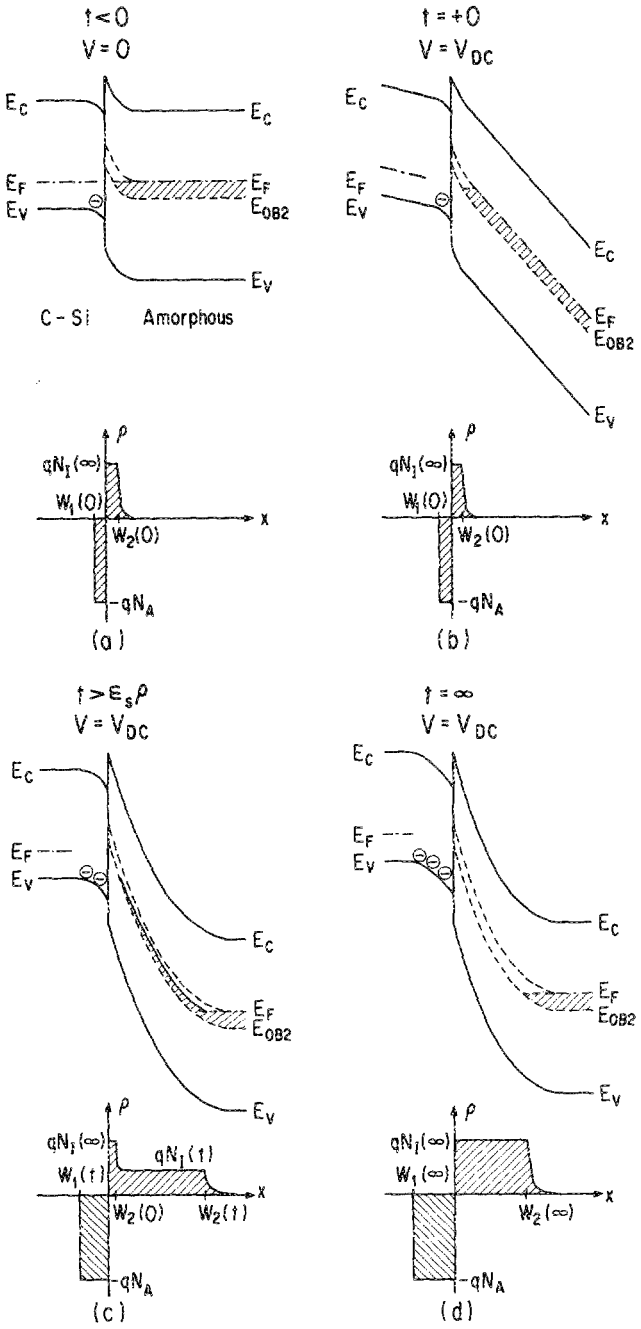

FIG. 2. Schematic sketches (energy-band diagram and space-charge density) of the heterojunction at four different times. In energy-band diagrams, the gap states as indicated by the hatched area are occupied by electrons so that they are neutral. In the depletion region, therefore, the empty gap states between E_F and E_{OB2} behave like positively charged states. Dashed-dotted lines represent the Fermi level. ⊖ represents negatively charged acceptors in the depletion region.

and crystalline components, as shown in Fig. 2(b). Electrons trapped at shallower states at $t<0$ get thermally emitted into the conduction band. After the applied bias has been on for the dielectric relaxation time of the amorphous film,[20] the space charge in the vicinity of the heterojunction will redistribute itself in response to the applied potential, as shown in Fig. 2(c). The data of HMC after the dielectric relaxation time can be analyzed from Eq. (10), and N_I at a time of t can be expressed as

$$N_I(t)=\epsilon_{s1}V_c(t)N_A/\epsilon_{s2}[V_B-V_{DC}-V_c(t)], \quad (11)$$

with

$$V_c(t)=qN_AW_1^2(t)/2\epsilon_{s1} \quad (12)$$

and

$$W_1(t)=\epsilon_{s1}[1/C_{HM}(t)-1/C_2], \quad (13)$$

where $W_1(t)$ is the depletion width at time t and $V_c(t)$ is the voltage across the depletion region of c-Si at t. In order to make the above analysis feasible, the absolute value of V_{DC} has to be necessarily much higher than V_B, so that the relation $[N_I(t)W_2(t)\gg N_I(\infty)W_2(0)]$ is valid and the average value of N_I over the depletion region at t is close to $N_I(t)$. This condition also suggests that interface states do not affect the measurement of HMC.

The function $H(t)$ is defined as

$$H(t)\equiv -t\left(\frac{d\Delta N_I(t)}{dt}\right), \quad (14)$$

with

$$\Delta N_I(t)\equiv N_I(t)-N_I(\infty). \quad (15)$$

Under the conditions that the emission rate (e_n) for electrons is much higher than that (e_p) for holes and the Fermi–Dirac distribution function $f(E)$ is close to unity (i.e., for the gap states between E_F and E_{OB2}), the relations

$$g[E(t)]=H(t)/kT \quad (16)$$

and

$$E_C-E(t)=kT\ln(\nu_n t), \quad (17)$$

are obtained (see Appendix B), which are similar to the relations obtained from the ICTS analysis.[12]

On the other hand, $H(t)$ is theoretically derived (see Appendix A) as

$$H(t)=\int_{E_V}^{E_C}[f(E)-F_\infty(E)]g(E)t[e_n(E)+e_p(E)]\times\exp\{-[e_n(E)+e_p(E)]t\}\,dE, \quad (18)$$

with

$$f(E)=1/\{1+\exp[(E-E_F)/kT]\}, \quad (19)$$

$$F_\infty(E)=e_p(E)/[e_n(E)+e_p(E)], \quad (20)$$

$$e_n(E)=\nu_n\exp[(E-E_C)/kT], \quad (21)$$

and

$$e_p(E)=\nu_p\exp[(E_V-E)/kT]. \quad (22)$$

The method of determining $g(E)$ from which $H(t)$ of Eq. (18) can be obtained to fit the measured $H(t)$, has been described in Sec. IV B. Although the application of the transient HMC method to an isothermal mode like ICTS is only discussed in this paper, this method can also be applied to a temperature-scanning mode like DLTS.

III. PREPARATION AND FILM PROPERTIES

Undoped a-Si:H and a-$Si_{1-x}Ge_x$:H films have been deposited by inductively coupled glow-discharge decomposition of pure SiH_4 gas and $GeH_4/SiH_4/H_2$ gas mixture, respectively, and a relation between the flowrates and the

TABLE I. Relationship between flowrates and optical gap.

Flowrate (sccm) \ Optical gap (eV)	1.30	1.44	1.52	1.60	1.70
5% GeH_4 in H_2	10	7	6	5	0
Pure SiH_4	1	1	1	1	5

optical gap (E_0) determined by the Tauc plots is shown in Table I. Gas pressure of 50 mTorr and rf power of 5 W have been maintained during the deposition.

Figure 3 shows the dark conductivity (σ_d) and photoconductivity ($\Delta\sigma_{ph}$) of the films (about 0.5-μm thickness) deposited onto Corning 7059 glass substrates heated to 200 °C. The other properties of the films are shown in Table II.

The heterojunctions have been fabricated by depositing the amorphous films onto four kinds of p c-Si substrates of different resistivities heated to 200 °C and then evaporating magnesium (Mg) on these films at room temperature. Mg forms an ohmic contact with undoped a-Si:H as well as undoped a-$Si_{1-x}Ge_x$:H.[21,23] Thicknesses of a-Si:H and a-$Si_{1-x}Ge_x$:H have been kept between 0.8 and 1.2 μm. Heterojunctions with p c-Si having resistivity less than 0.01 Ω cm have been used to make sure that the capacitances are independent of the applied bias, as described in Eq. (6). The values of N_A for the other three p c-Si are 7.8×10^{14}, 1.0×10^{16}, and 3.5×10^{16} cm^{-3}. All the heterojunctions have exhibited good rectifying properties.

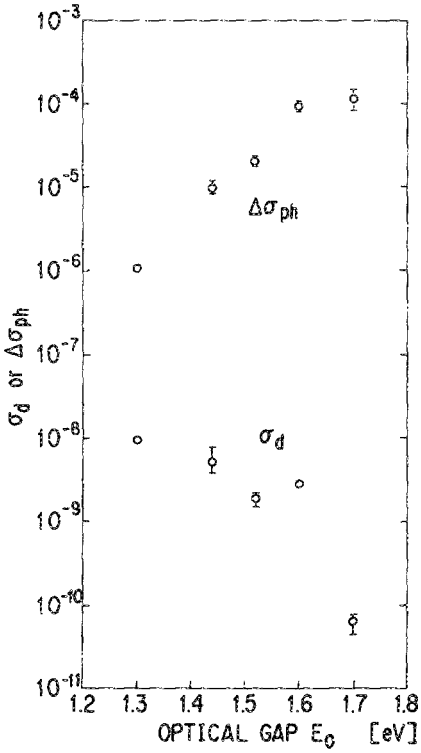

FIG. 3. Dark conductivity (σ_d) and photoconductivity ($\Delta\sigma_{ph}$) under AM1 and 100 mW/cm^2 of undoped films with various optical gaps.

TABLE II. Film properties of a-$Si_{1-x}Ge_x$:H and a-Si:H used in this study. E_0: Optical gap; δ_2: Activation energy of dark conductivity; E_u: Urbach energy obtained from CPM.

Material	a-$Si_{1-x}Ge_x$:H				a-Si:H
Sample number	40279	40278	40276	40274	40272
E_0 (eV)	1.30	1.44	1.52	1.60	1.70
δ_2 (eV)	0.64	0.65	0.66	0.69	0.73
E_u (meV)	59	55	55	61	45

IV. RESULTS AND DISCUSSION

A. Steady-state HMC measurements

C-V characteristics of the heterojunctions have been measured at 1 MHz at room temperature. Since thermal-emission rates of electrons from the traps to the conduction band are usually lower than capture rates of electrons from the conduction band into the traps in the case of undoped a-Si:H and a-$Si_{1-x}Ge_x$:H, the capacitance should be measured from a higher reverse bias to a lower bias. The sweep rate (dV_{DC}/dt) should be small. For example, the sweep rates in this study have been about 0.004 V/s. Figure 4 shows the $W_I^2 - V_{DC}$ characteristics obtained using Eq. (9) from C-V characteristics of the a-$Si_{1-x}Ge_x$:H ($E_0 = 1.52$ eV)/p c-Si ($N_A = 1.0\times10^{16}$ cm^{-3}) heterojunction. The value of C_2 which has been used to calculate W_I in Eq. (9) is the saturated capacitance with the forward bias. The data reveal a good linear relationship, indicating that the model mentioned in Sec. II A is applicable to the present system. As is clear from Eq. (10), magnitudes of N_I and V_B can be graphically determined from the slope and the intercept of the abscissa, respectively. Values of $N_I = 1.3\times10^{16}$ cm^{-3} and $V_B = 0.48$ eV have been obtained from Fig. 4. It has been experimentally found that the $W_I^2 - V_{DC}$ relations for all the heterojunctions obey Eq. (10). The dependence of N_I on E_0 is shown in Fig. 5.

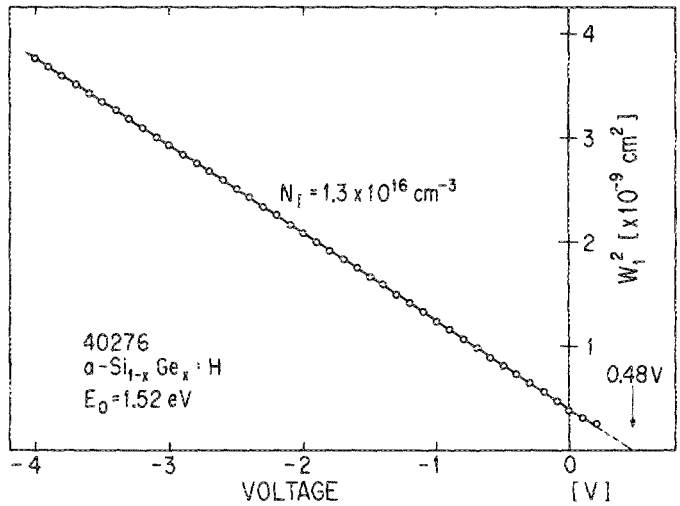

FIG. 4. Width of the depletion region in p c-Si ($N_A = 1.0\times10^{16}$ cm^{-3}) as a function of dc voltage for a-$Si_{1-x}Ge_x$:H ($E_0 = 1.52$ eV).

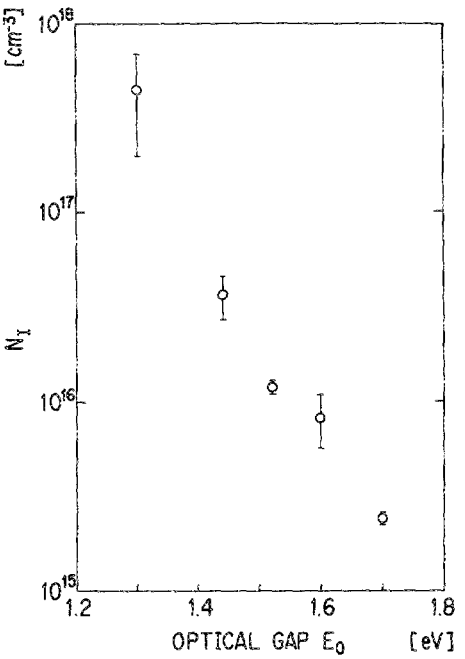

FIG. 5. Effective density of donorlike states as a function of optical gap.

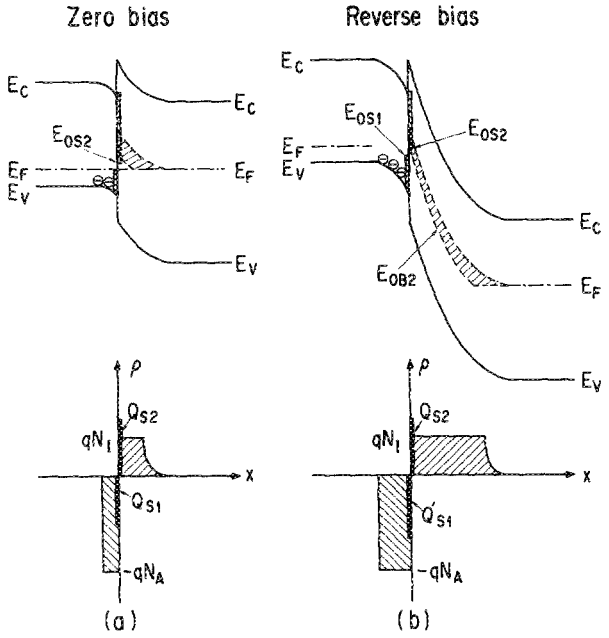

FIG. 6. Schematic sketches of the heterojunction in order to understand the effect of interface states. According to the energy-band diagram, the total charge Q_{S2} of positively charged interface states in the amorphous film is independent of the reverse bias because E_{OS2} is above E_F in the amorphous film even at zero bias. The total charge of negatively charged interface states in c-Si increases with the reverse bias until E_{OS1} becomes below E_F in c-Si, and then it attains a constant value Q'_{S1}. Dashed-dotted lines represent the Fermi level. ⊖ represents negatively charged acceptors in the depletion region.

The problem of interface states seems important and unavoidable in the present heterojunction system because interface states between amorphous and crystalline semiconductors may affect the C-V characteristics. Two kinds of interface states have been considered; one is an acceptorlike interface state in p c-Si and the other is a donorlike interface state in the amorphous film. Since a reverse current flows across these heterojunctions, the energies (E_{OS1} and E_{OS2}) shown in Fig. 6 are defined as follows. When free carriers near the interface are depleted, there exists a maximum energy level (E_{OS1}) below which the interface states behave like negatively charged states in p c-Si, and there is a minimum energy level (E_{OS2}) above which the interface states behave like positively charged states in the amorphous film, as is similar to the case of the depletion region in amorphous semiconductors mentioned in Sec. II A. Each energy level is probably located near the middle of their respective band gaps. Since the position of the Fermi level in undoped a-Si:H and a-$Si_{1-x}Ge_x$:H is located in an energy close to the midgap position, E_{OS2} is above E_F at the interface even at the zero-bias condition. This indicates that the total charge Q_{S2} of positively charged interface states in the amorphous film does not depend on the reverse-bias voltage so that Q_{S2} is constant, as shown in Fig. 6. Although the total charge Q_{S1} of negatively charged interface states in p c-Si increases with the reverse bias, it attains a constant value Q'_{S1} when E_{OS1} is below E_F in c-Si. Therefore, N_I determined at high reverse bias is reliable even if the interface states exist.

Although interface state densities depend on the condition of the p c-Si component, the experimental results of N_I determined from the heterojunctions using p c-Si wafers having motley resistivity values and orientations show only a little scatter, suggesting that the values of N_I obtained, are representative of the bulk unaffected by interface states. The magnitude of N_I obtained for undoped a-Si:H ($E_0 = 1.70$ eV) is 2.4×10^{15} cm^{-3}, and this remains unaltered at measuring frequencies higher than 1 kHz and at measuring temperatures lower than 353 K.

Besides the interface states, it has been reported that there is a qualitatively different layer ($\sim$50 Å) near the interface from the bulk.[24] This layer near the interface affects the capacitance. However, N_I is estimated from the increment of the depletion width in the amorphous film with the reverse bias. Since the region where the depletion width increases at high reverse bias is far from the interface, N_I obtained at high reverse bias is unaffected by this layer near the interface.

N_I values for $E_0 = 1.70$ and 1.30 eV are close to the spin densities obtained by electron-spin-resonance measurements (ESR). The g values obtained are 2.0055 and 2.018 for $E_0 = 1.70$ and 1.30 eV, respectively. The density of paramagnetic defect centers is obtained from ESR, and the determined g values suggest that dominant singly occupied dangling bonds (D^0) for $E_0 = 1.70$ and 1.30 eV are formed by silicon atoms and germanium atoms, respectively.[25] These results indicate that N_I represents the density of gap states below the Fermi level, and also that most of the gap states are singly occupied dangling bonds.

The steady-state HMC method provides a simple process to determine the density of gap states near the midgap, and these results have been found to be reliable.

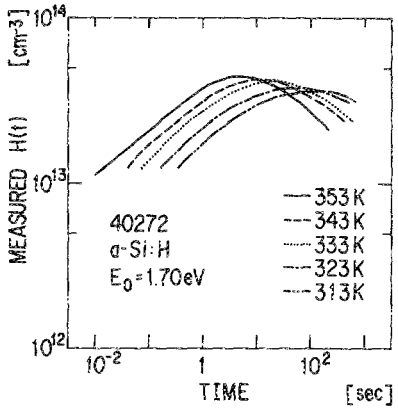

FIG. 7. Signals of $H(t)$ obtained experimentally from HMC with p c-Si ($N_A = 7.8\times10^{14}$ cm^{-3}) at five different temperatures for a-Si:H ($E_0 = 1.70$ eV). (50-s filling time, 4-V reverse bias.)

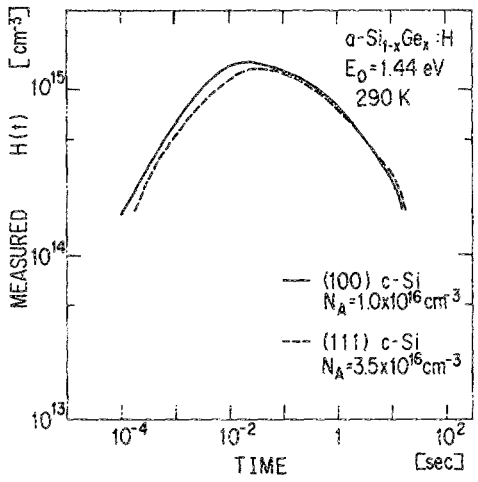

FIG. 9. Set of two measured $H(t)$ corresponding to (111) and (100) surfaces of c-Si for a-Si$_{1-x}$Ge$_x$:H ($E_0 = 1.44$ eV). (50-s filling time, 4-V reverse bias.)

B. Transient HMC measurements

Transient HMC measurements have been carried out at 2 MHz at various temperatures. Only signals of $H(t)$ longer than the dielectric relaxation time are valid, however, as mentioned in Sec. II B. The experimental results of $H(t)$ for undoped a-Si:H ($E_0 = 1.70$ eV) and a-Si$_{1-x}$Ge$_x$:H ($E_0 = 1.52$ eV) are shown in Figs. 7 and 8, respectively. The signals of $H(t)$ get saturated at a filling time (under the zero-bias condition) longer than 1 s. $H(t)$ has been measured at a filling time of 50 s. The signal of $H(t)$ has been found to be independent of V_{DC} for $V_{DC} < -3$ V, while it has been found to vary with V_{DC} for $V_{DC} > -3$ V. This indicates that the effect of interface states is eliminated at $V_{DC} < -3$ V. Therefore, the transient HMC was measured at -4 V.

In order to check to what extent the interface states can affect the signal of $H(t)$, the signals of $H(t)$ with different surfaces of c-Si have been compared, as shown in Fig. 9. The (111) surface of c-Si has the largest number of available bonds per cm^2, and the (100) surface has the smallest. According to the experimental results from Si/SiO$_2$ systems,[26,27] the interface state density for the (100) surface was found to be lower by a factor of 10 compared to that for the (111) surface. However, in the present work, $H(t)$ has not shown variation with surface orientation. Moreover, $H(t)$ has been found to be independent of the resistivity of p c-Si. Thus, from these experimental results of steady-state and transient HMC, and also the consideration mentioned in Sec. II B, $H(t)$ may be considered to be unaffected by the interface states.

In order to calculate $H(t)$ using Eq. (18), only ν_n and ν_p are necessary. The electron thermal-emission rate $e_n(E)$

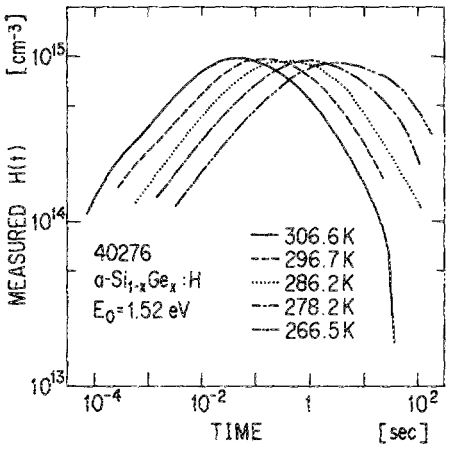

FIG. 8. Signals of $H(t)$ obtained experimentally from HMC with p c-Si ($N_A = 1.0\times10^{16}$ cm^{-3}) at five different temperatures for a-Si$_{1-x}$Ge$_x$:H ($E_0 = 1.52$ eV). (50-s filling time, 4-V reverse bias.)

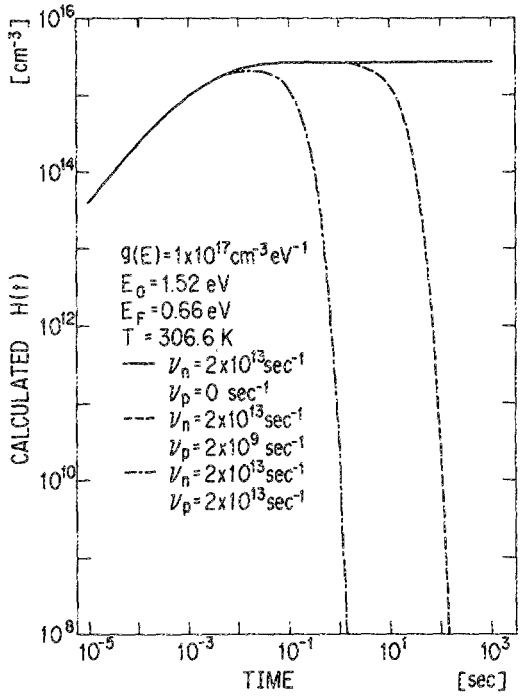

FIG. 10. Set of three calculated $H(t)$ corresponding to different attempt-to-escape frequencies for holes with $g(E) = 1\times10^{17}$ cm^{-3} eV^{-1} and $\nu_n = 2\times10^{13}$ s^{-1} for $E_0 = 1.52$ eV.

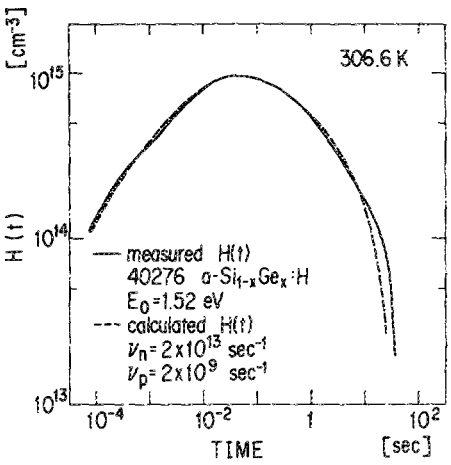

FIG. 11. Comparison between the measured $H(t)$ for a-$Si_{1-x}Ge_x$:H ($E_0 = 1.52$ eV) and the calculated $H(t)$ with $E_{g2} = 1.52$ eV, $\nu_n = 2\times10^{13}$ s^{-1}, and $\nu_p = 2\times10^9$ s^{-1}.

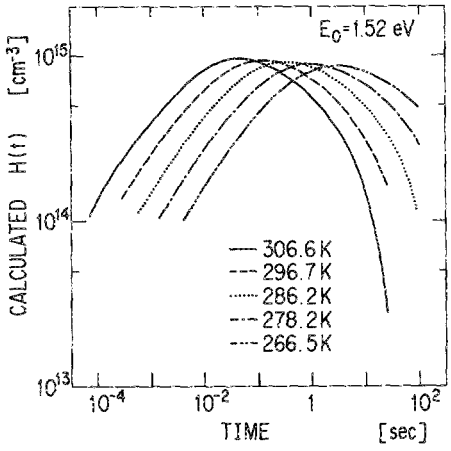

FIG. 13. Calculated $H(t)$ for $E_0 = 1.52$ eV with $E_{g2} = 1.52$ eV, $\nu_n = 2\times10^{13}\,s^{-1}$, and $\nu_p = 2\times10^9\,s^{-1}$. These curves fit the measured $H(t)$ at each temperature well.

for a particular trap level at a depth $(E_C - E)$ from the conduction band is given by Eq. (21), and the time, which is required for a trapped electron to be thermally re-emitted, is $1/e_n(E)$. Under the assumption that the gap states corresponding to the peak of $H(t)$ is located between E_F and E_{OB2}, $g(E_{\text{peak}})$ is obtained as $H(t_{\text{peak}})/kT$ from Eq. (16). Therefore, the values of ν_n can be approximately estimated from the temperature dependence of the time (t_{peak}) at the peak of $H(t)$. Then,

$$t_{\text{peak}} = 1/e_n(E_{\text{peak}}) = (1/\nu_n)\exp[(E_C - E_{\text{peak}})kT], \quad (23)$$

if ν_n is independent of temperature and energy. Moreover, a maximum value of ν_p/ν_n is estimated as follows. Figure 10 shows the calculated $H(t)$ for different ν_p with $g(E) = 1\times10^{17}$ $cm^{-3}\,eV^{-1}$ and $\nu_n = 2\times10^{13}$ s^{-1}. In the case of $\nu_p/\nu_n = 1$ using $E_{g2} = E_0 = 1.52$ eV, the measured $H(t)$ at 1.4 s (306.6 K) have been found to be about 5×10^{14} cm^{-3} from Fig. 8, and the calculated one about 10^8 cm^{-3} from Fig. 10, suggesting that the value of $g(E)$ at E, corresponding to 1.4 s, should attain an unbelievable value of 5×10^{23} $cm^{-3}\,eV^{-1}$. From the above consideration, the value of ν_n and the maximum value of ν_p have been taken as 2×10^{13} and 2×10^9 s^{-1}, respectively, and the calculated $H(t)$ have been found to fit the measured $H(t)$ very well as shown in Fig. 11. Here, $g(E)$ as shown in Fig. 12 has been used, and it has been assumed that the mobility gap E_{g2} ($= E_C - E_V$) coincides with E_0.[28] Figure 13 shows the temperature dependence of the calculated $H(t)$ which fits the measured $H(t)$ at each temperature. The $g(E)$ for a-Si:H and a-$Si_{1-x}Ge_x$:H ($E_0 = 1.60$, 1.44, and 1.30 eV) are shown in Figs. 14–17 using maximum values of ν_p.

Integrated $g(E)$ for each sample has been found to be correlated with N_I although it is marginally smaller than N_I. Therefore, $g(E)$ mainly represents the distribution of D^0.

The distribution $g(E)$ that has been obtained is found to be the bulk DOS distribution unaffected by interface states. This appears to be the first systematic effort to electrically estimate $g(E)$ below the Fermi level for undoped amorphous semiconductors using heterojunctions with crystalline semiconductors. Therefore, the author has considered the validity of this HMC method in more detail. The following pertinent questions could arise, viz.,

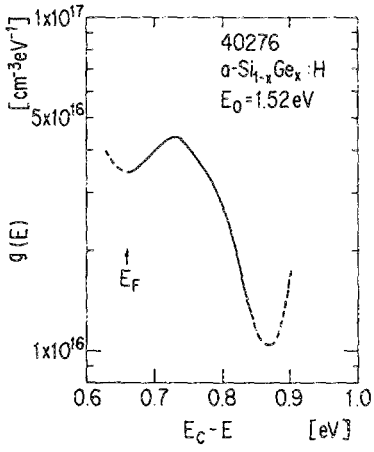

FIG. 12. Density of states for a-$Si_{1-x}Ge_x$:H ($E_0 = 1.52$ eV).

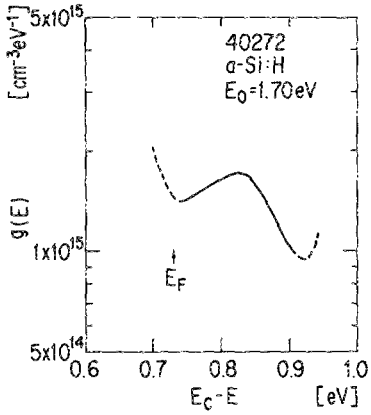

FIG. 14. Density of states for a-Si:H ($E_0 = 1.70$ eV) from which the calculated $H(t)$ can be obtained to fit the measured $H(t)$ with $E_{g2} = 1.70$ eV, $\nu_n = 1\times10^{11}\,s^{-1}$, and $\nu_p = 1\times10^8\,s^{-1}$.

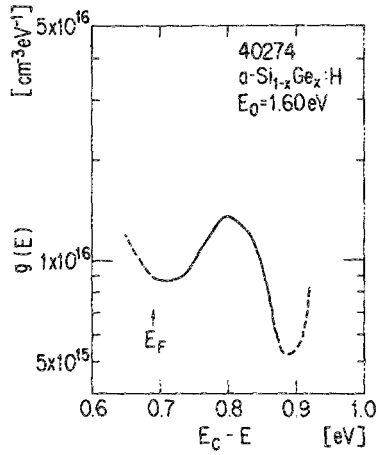

FIG. 15. Density of states for a-$Si_{1-x}Ge_x$:H ($E_0 = 1.60$ eV) from which the calculated $H(t)$ can be obtained to fit the measured $H(t)$ with $E_{g2} = 1.60$ eV, $\nu_n = 2\times10^{13}$ s^{-1}, and $\nu_p = 5\times10^{9}$ s^{-1}.

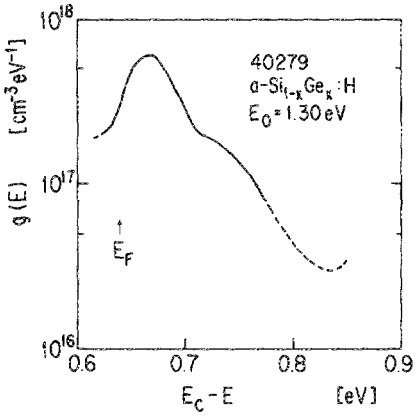

FIG. 17. Density of states for a-$Si_{1-x}Ge_x$:H ($E_0 = 1.30$ eV) from which the calculated $H(t)$ can be obtained to fit the measured $H(t)$ with $E_{g2} = 1.30$ eV, $\nu_n = 3\times10^{14}$ s^{-1}, and $\nu_p = 5\times10^{7}$ s^{-1}.

(1) Is the assumption that ν_n and ν_p are independent of temperature and energy correct?

(2) Are the values obtained for ν_n and ν_p reasonable?

(3) To what degree does tunneling affect $g(E)$?

There has been a controversy in opinion regarding the answers to (1) and (2) mainly on the basis of results obtained from DLTS[8–10] and ICTS.[11,12] These techniques have mainly been applied to phosphorus (P)-doped a-Si:H, but few data exist for undoped a-Si:H and a-$Si_{1-x}Ge_x$:H.

If the ν_n has a temperature dependence of the form[29]

$$\nu_n = \nu_{n0} T^2 \exp(-\Delta E_a/kT), \tag{24}$$

where ν_{n0} is a constant independent of T, Eq. (23) changes into

$$t_{\text{peak}} = (1/\nu_{n0} T^2)\exp[(E_C - E_{\text{peak}} + \Delta E_a)/kT], \tag{25}$$

indicating that the energies shown in Figs. 12 and 14–17 are overestimated because of the assumption that $\Delta E_a = 0$. The situation is the same as that reported by Lang and Cohen.[10]

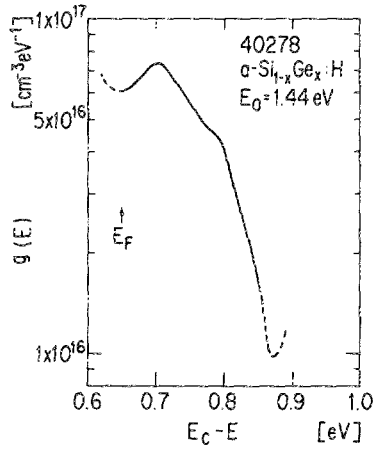

FIG. 16. Density of states for a-$Si_{1-x}Ge_x$:H ($E_0 = 1.44$ eV) from which the calculated $H(t)$ can be obtained to fit the measured $H(t)$ with $E_{g2} = 1.44$ eV, $\nu_n = 1\times10^{14}$ s^{-1}, and $\nu_p = 1\times10^{8}$ s^{-1}.

Therefore, it is important to investigate the temperature dependence of ν_n. The author has tried to estimate it by means of the trap filling method like ICTS,[12] but difficulty has been encountered owing to the long dielectric relaxation time of amorphous films. However, the energy locations of the peak of DOS (probably D^0) for undoped materials have been found to be close to those reported by Tsutsumi *et al.*[30] and Kocka, Vanecek, and Schaver.[31] However, the positions are shallower than those reported by Mori, Okushi, and Tanaka.[32]

The value of ν_p estimated from the fitting procedure depends strongly on the mobility gap (E_{g2}) because e_p depends on $(E_C - E) - E_{g2}$. The $g(E)$ estimated with $\nu_n = \nu_p = 1\times10^{11}$ s^{-1} and $E_{g2} = 1.91$ eV is the same as the $g(E)$ shown in Fig. 14 with $\nu_n = 1\times10^{11}$ s^{-1}, $\nu_p = 1\times10^{8}$ s^{-1}, and $E_{g2} = 1.7$ eV because E_{OB2} is the same in both cases. The value of the mobility gap poses an open question.[33] Vanecek *et al.*[33] concluded that the mobility gap of a-Si:H was quite close to E_0. On the other hand, Lang and coworkers[9] have used values between 1.9 and 2.1 eV for the mobility gap of a-Si:H based on the assumption $\nu_p = \nu_n = 10^{13}$ s^{-1}. Jackson *et al.*[34] have reported it as 1.93 ± 0.2 eV. However, the estimated $g(E)$ does not change when the best fit is obtained using the maximum of ν_p/ν_n, which is determined by the value of E_{g2}.

Regarding the third question, it seems that tunneling does not affect $g(E)$ in the range of the measuring temperatures from considerations similar to the ICTS analysis of P-doped a-$Si_{1-x}Ge_x$:H.[35] However, more detailed work pertaining to these points is now in progress.

V. CONCLUSION

The auhtor has described a novel technique for determining the magnitude as well as energy location of midgap states in undoped a-Si:H and undoped a-$Si_{1-x}Ge_x$:H. The capacitance (HMC) of undoped a-Si:H (or a-$Si_{1-x}Ge_x$:H)/p c-Si heterojunctions has been measured at a frequency greater than the reciprocal of the dielectric relaxation time ($\epsilon_{s2}\rho_2$). The heterojunction-monitored capacitance is essentially the resultant of two capacitances in

series, formed in the c-Si and the amorphous film, respectively. The capacitance of the amorphous film is determined by the film thickness on account of its high resistivity, while that of c-Si follows from the depletion width of c-Si. The latter also reflects the space charge of the depletion region in the amorphous film.

The steady-state HMC method gives information on the density of gap states (mainly D^0) in the bulk of the amorphous film near the midgap. The transient HMC method, likewise, gives the DOS distribution near the midgap. Both methods have been found to be unaffected by interface states.

ACKNOWLEDGMENTS

The author wishes to acknowledge his gratitude to Dr. K. Tanaka, Dr. H. Okushi, and other members of the staff of the Amorphous Materials Section in the Electrotechnical Laboratory for their valuable insights and comments. He wishes to thank Dr. A. Matsuda for advice in the deposition of a-$Si_{1-x}Ge_x$:H. He wishes to express his gratitude to Dr. Z E. Smith from Princeton University for carrying out the CPM measurements and also for fruitful discussions. To S. Yokoyama, the author is grateful for measurements of ESR. He wishes to thank Dr. R. Banerjee for critical reading of the manuscript.

APPENDIX A

At thermal equilibrium (i.e., in the neutral region of the film), the densities $[n_T(E)$ and $p_T(E)]$ of traps $[g(E)]$ occupied by electrons and holes, respectively, are expressed as

$$n_T(E)/g(E) = f(E) \tag{A1}$$

and

$$g(E) = n_T(E) + p_T(E)\,, \tag{A2}$$

according to the Fermi–Dirac statistics, and Eq. (A1) is used in Eqs. (18) and (19) in the text.

A rate equation for capture and emission processes is given by

$$\frac{dn_T(E)}{dt} = n\sigma_n(E)v_{\rm th}p_T(E) - e_n(E)n_T(E) - p\sigma_p(E)v_{\rm th}n_T(E) + e_p(E)p_T(E)\,, \tag{A3}$$

where n and p are the concentrations for free electrons and free holes in the extended states, respectively, $\sigma_n(E)$ and $\sigma_p(E)$ are the capture cross sections for electrons and holes at E, respectively, and $v_{\rm th}$ is the thermal velocity. The condition $dn_T(E)/dt = 0$ holds for the steady state, and free electrons and free holes are swept out ($pn \ll n_i^2$) in the depletion region, where n_i is the intrinsic carrier density. Therefore, Eq. (20) in the text

$$F_\infty(E) = n_T(E)/g(E) = e_p(E)/[e_n(E) + e_p(E)]\,,$$

is obtained from Eqs. (A2) and (A3).

In the depletion region ($np \ll n_i^2$), Eq. (A3) can be rewritten as

$$\frac{dn_T(E)}{dt} = e_p(E)g(E) - [e_n(E) + e_p(E)]n_T(E)\,, \tag{A4}$$

using Eq. (A2), and this solution is

$$n_T(E;t) = [f(E) - F_\infty(E)]g(E) \times \exp\{-[e_n(E) + e_p(E)]t\} + e_p(E)g(E)/[e_n(E) + e_p(E)]\,, \tag{A5}$$

using the relation of $n_T(E;0) = f(E)g(E)$. Therefore,

$$\Delta N_t(t) = \int_{E_V}^{E_C} [n_T(E;t) - n_T(E;\infty)]\,dE = \int_{E_V}^{E_C} [f(E) - F_\infty(E)]g(E) \times \exp\{-[e_n(E) + e_p(E)]t\}\,dE\,, \tag{A6}$$

is obtained, and then Eq. (18) is derived from Eq. (A6) easily.

The energy E_{OB2} where $F_\infty(E_{OB2}) = 0.5$ is

$$E_{OB2} = E_C - \frac{E_{g2}}{2} + \left(\frac{kT}{2}\right)\ln\left(\frac{\nu_p}{\nu_n}\right), \tag{1}$$

from Eqs. (20)–(22) in the text. In the depletion region, traps below E_{OB2} are occupied by electrons and traps above E_{OB2} are empty.

In the case of metal-insulator-semiconductor diodes, a current does not flow across the junction, which means that the Fermi level can be defined even in the depletion region because the quasi-Fermi level for electrons coincides with the quasi-Fermi level for holes. Therefore, a relation $np = n_i^2$ in the depletion region is valid and $n_T(E)/g(E)$ coincides with $f(E)$, indicating that the energy of E_{OB2} cannot be defined. Equations (1) and (20) in the text are valid only when a current flows across the junction, i.e., the quasi-Fermi level for electrons, does not coincide with the quasi-Fermi level for holes in the depletion region.

APPENDIX B

Under the conditions that $e_n \gg e_p$ and $f(E) \sim 1$, Eq. (18) in the text is rewritten as

$$H(t) = \int_{E_V}^{E_C} g(E)D(E;t)\,dE\,, \tag{B1}$$

where

$$D(E;t) = e_n(E)t\exp[-e_n(E)t]\,. \tag{B2}$$

The function $D(E;t)$ is maximum at $e_n(E)t = 1$ and can be approximated using a delta function as

$$D(E;t) \simeq kT\delta(E - E_m)\,, \tag{B3}$$

where E_m is the energy at which $D(E;t)$ takes a maximum value when $e_n(E_m)t_m = 1$. The relation between E_m and t_m is derived from Eq. (21) as follows:

$$E_C - E_m = kT\ln(\nu_m t_m)\,. \tag{B4}$$

In a more general form, i.e., for the case of continuously distributed gap states within the energy gap, the equation

can be expressed as

$$E_C - E(t) = kT \ln(\nu_n t) . \quad (17)$$

From Eqs. (B1) and (B3), the relationship between $H(t)$ and $g(E)$ is obtained as

$$g[E(t)] = H(t)/kT . \quad (16)$$

[1]S. Yamasaki, K. Nakagawa, H. Yamamoto, A. Matsuda, H. Okushi, and K. Tanaka, in *Tetrahedrally Bonded Amorphous Semiconductors*, edited by R. A. Street, D. K. Biegelsen, and J. C. Knights (American Institute of Physics, New York, 1981), p. 258.

[2]S. Yamasaki, H. Hata, T. Yoshida, H. Oheda, A. Matsuda, H. Okushi, and K. Tanaka, J. Phys. **42**, C4–297 (1981).

[3]S. Yamasaki, H. Oheda, A. Matsuda, H. Okushi, and K. Tanaka, Jpn. J. Appl. Phys. **21**, L539 (1982).

[4]S. Yamasaki, Philos. Mag. B **56**, 79 (1987).

[5]W. B. Jackson and N. M. Amer, J. Phys. **42**, C4–293 (1981).

[6]N. M. Amer and W. B. Jackson, in *Semiconductors and Semimetals*, edited by J. I. Pankove (Academic, Orlando, FL, 1984), Vol. 21, part B, p. 83.

[7]M. Vanecek, J. Kocka, J. Stuchlik, Z. Kozisek, O. Stika, and A. Triska, Sol. Energy Mater. **8**, 411 (1983).

[8]J. D. Cohen, D. V. Lang, and J. P. Harbison, Phys. Rev. Lett. **45**, 197 (1980).

[9]D. V. Lang, J. D. Cohen, and J. P. Harbison, Phys. Rev. B **25**, 5285 (1982).

[10]J. D. Cohen and D. V. Lang, Phys. Rev. B **25**, 5321 (1982).

[11]H. Okushi, Y. Tokumaru, S. Yamasaki, H. Oheda, and K. Tanaka, Jpn. J. Appl. Phys. **20**, L549 (1981).

[12]H. Okushi, Philos. Mag. B **52**, 33 (1985).

[13]H. Oheda, S. Yamasaki, T. Yoshida, A. Matsuda, H. Okushi, and K. Tanaka, Jpn. J. Appl. Phys. **21**, L440 (1982).

[14]Y. Nitta, K. Abe, K. Hattori, H. Okamoto, and Y. Hamakawa, J. Non-Cryst. Solids **97/98**, 695 (1987).

[15]K. D. Mackenzie, P. G. LeComber, and W. E. Spear, Philos. Mag. B **46**, 377 (1982).

[16]I. Solomon and R. Benferhat, Phys. Rev. B **30**, 3422 (1984).

[17]F. Schaver and J. Kocka, Philos. Mag. B **52**, L25 (1985).

[18]H. Matsuura, T. Okuno, H. Okushi, and K. Tanaka, J. Appl. Phys. **55**, 1012 (1984).

[19]Since the total charge of positively charged gap states is close to $qN_t W_2$, W_2 can be called the depletion width of the amorphous semiconductor though W_2 is not equal to the exact depletion width.

[20]In the case of undoped amorphous materials, the drift time ($L^2/\mu V$) is shorter than the dielectric relaxation time ($\epsilon_{s2}\rho_2$) where ρ_2 is the dark conductivity in the bulk and μ the mobility of electrons. Therefore, all the free electrons in the amorphous film are swept out before $\epsilon_{s2}\rho_2$, and the resistivity becomes higher than ρ_2. There are some arguments that the resistivity corresponding to n_i should be used to estimate the dielectric relaxation time, where n_i is the intrinsic carrier density which represents a density of thermally generated carriers [for example, see H. Okushi, Jpn. J. Appl. Phys. **18**, 791 (1979)]. Fortunately, the dielectric relaxation time can be considered as $\epsilon_{s2}\rho_2$, since electron densities of undoped materials in this study are thought to be close to their n_i.

[21]H. Matsuura, T. Okuno, H. Okushi, S. Yamasaki, A. Matsuda, N. Hata, H. Oheda, and K. Tanaka, Jpn. J. Appl. Phys. **22**, L197 (1983).

[22]H. Matsuura, A. Matsuda, H. Okushi, T. Okuno, and K. Tanaka, Appl. Phys. Lett. **45**, 433 (1984).

[23]H. Matsuura and H. Okushi, J. Appl. Phys. **62**, 2871 (1987).

[24]R. W. Collins and J. M. Cavese, J. Non-Cryst. Solids **97/98**, 269 (1987).

[25]T. Shimizu, M. Kumeda, and Y. Kiriyama, Solid State Commun. **37**, 699 (1981).

[26]P. V. Gray and D. M. Brown, Appl. Phys. Lett. **8**, 31 (1966).

[27]M. H. White and J. R. Cricchi, IEEE Trans. Electron Devices **ED-19**, 1280 (1972).

[28]The assumption of $\nu_n = \nu_p = 2\times 10^{13}\ s^{-1}$ requires that E_{g2} be 1.76 eV for the film with $E_0 = 1.52$ eV. However, $g(E)$ estimated using these values is the same as $g(E)$ shown in Fig. 12.

[29]A well-known expression derived from detailed balance arguments relates ν_n to these more fundamental parameters, namely, $\nu_n = \sigma_n v_{th} N_C$, where σ_n is the electron-capture cross section of gap states, v_{th} is the average thermal velocity of conduction electrons, and N_C is the effective density of states in the conduction band. The term of T^2 in Eq. (24) comes from the temperature dependence of $v_{th}N_C$, and the term of $\exp(-\Delta E_a/kT)$ results from the temperature dependence of σ_n [for example, see C. H. Henry and D. V. Lang, Phys. Rev. B **15**, 989 (1977)]. The variation of T^2 can be neglected in the temperature range used in this study. There is no information on ΔE_a for a-Si:H and a-$Si_{1-x}Ge_x$:H. In the present stage, however, it is probable to assume $\Delta E_a = 0$ partly because ΔE_a for crystalline semiconductors is usually reported to be zero [for example, see D. V. Lang and R. A. Logan, J. Electron. Mater. **4**, 1053 (1975)] and partly because Lang and co-workers (Ref. 9) assumed $\Delta E_a = 0$ for a-Si:H.

[30]Y. Tsutsumi, S. Sakata, K. Abe, Y. Nitta, H. Okamoto, and Y. Hamakawa, J. Non-Cryst. Solids **97/98**, 1063 (1987).

[31]J. Kocka, M. Vanecek, and F. Schaver, J. Non-Cryst. Solids **97/98**, 715 (1987).

[32]K. Mori, H. Okushi, and K. Tanaka, J. Non-Cryst. Solids **97/98**, 723 (1987).

[33]M. Vanecek, J. Stuchlik, J. Kocka, and A. Triska, J. Non-Cryst. Solids **77/78**, 299 (1985).

[34]W. B. Jackson, S. M. Kelso, C. C. Tsai, J. W. Allen, and S.-J. Oh, Phys. Rev. B **31**, 5187 (1985).

[35]H. Matsuura, H. Okushi, and K. Tanaka, J. Non-Cryst. Solids **97/98**, 963 (1987).